Comparison of giant dipole resonance decay in stiff ^{92}Mo and soft ^{100}Mo excited nuclei

M. Kicińska-Habior
Institute of Experimental Physics, University of Warsaw, 00-681 Warsaw, Poland and Nuclear Physics Laboratory, University of Washington, Seattle, Washington 98195

K. A. Snover, J. A. Behr,* C. A. Gossett, J. H. Gundlach, and G. Feldman†
Nuclear Physics Laboratory, University of Washington, Seattle, Washington 98195
(Received 24 September 1991)

Gamma-ray spectra from the decay of the giant dipole resonance (GDR) built on excited states of ^{92}Mo and ^{100}Mo nuclei at average spins(9-24)$\hbar$ and temperatures of 1.35–1.50 MeV were measured, and the parameters of a two-component GDR strength function were extracted. Deformations determined from the fitted component energies are substantially larger than predicted by the rotating liquid drop model, suggesting large thermal shape fluctuations. Widths of the GDR in ^{92}Mo increase from 7.6±0.1 to 8.6±0.2 MeV in the spin range of (9-19.5)$\hbar$ and temperature range of 1.35–1.45 MeV, as compared with the ground-state GDR width of 5.4±0.2 MeV. In ^{100}Mo the GDR width is nearly constant and equals 9.8±0.2, 9.9±0.2, and 10.1±0.2 MeV at average spins 9$\hbar$, 19.5$\hbar$ and 24$\hbar$ and temperatures 1.35, 1.45, and 1.50 MeV, respectively, as compared with the ground-state width of 7.9±0.2 MeV. The observed difference in the GDR widths between the two molybdenum isotopes at the same temperatures and spins indicates that shell effects are still present at the temperatures studied.

PACS number(s): 23.20.−q, 24.30.Cz, 27.50.+e

I. INTRODUCTION

Recent studies of high-energy γ-ray spectra [1–6] following the decay of the giant dipole resonance (GDR) built on highly excited states formed in heavy-ion fusion reactions have shown that the GDR strength function provides information on the deformation of the ensemble of excited nuclear states populated by the γ decay. These results motivated our interest in studying the GDR strength function for excited nuclei which are spherical vibrators in their ground states and hence undergo large quadrupole surface vibrations.

For these studies we chose even isotopes of molybdenum: ^{92}Mo and ^{100}Mo. Comparison of the GDR strength function for decay of ^{92}Mo* and ^{100}Mo* is particularly interesting because ^{92}Mo is a relatively stiff, nearly spherical nucleus close in mass to the quasimagic nucleus ^{90}Zr, while ^{100}Mo is a strong vibrator [7]. These nuclei, then, offer the opportunity to compare the temperature and spin broadening of the GDR in nuclei which, as a result of shell structure, have very different low-temperature softness. It is generally expected that at temperatures $T \sim 2$ MeV shell effects should be mostly dissolved [8]. A comparison of GDR decay in hot ^{92}Mo* and ^{100}Mo* compound nuclei for $T < 2$ MeV should provide information on the dissolution of shell effects with temperature.

The GDR built on the ground states of even molybdenum isotopes (A = 92–100) has been observed in the (γ, n) reaction [9]. It was found experimentally [9] that the ground-state GDR width in Mo isotopes is strongly dependent on the softness of the nucleus and increases from 5.4±0.2 MeV for ^{92}Mo to 7.9±0.2 MeV for ^{100}Mo. Data for the (γ,γ') reaction on ^{92}Mo and ^{96}Mo [10] are in good agreement with the dynamic collective model [10, 11], which involves a coupling between the zero-temperature quadrupole surface vibration and the GDR.

We used the ^{16}O + ^{76}Se and ^{18}O + ^{82}Se reactions to produce ^{92}Mo* and ^{100}Mo* compound nuclei such that, following GDR γ decay, the ensemble of states has the same effective temperatures T_f=1.35–1.50 MeV and the same average final spins $\bar{I}$=(9–24)$\hbar$ (see Table I). The parameters of the GDR strength function were extracted from fits of the statistical model calculations to the measured γ-ray spectra at θ_γ=90°. The level densities in the Reisdorf parametrization [12] with parameters appropriate for nuclei with mass $A \approx 90 - 100$ [4] were used. Some results obtained with level densities in the Pühlhofer parametrization [13] are also discussed. All measured spectra were reproduced by statistical calculations with a two-component GDR strength function. Because the deformation splitting of the GDR was not resolved, calculations with a one-component GDR strength function were also performed.

II. EXPERIMENT DETAILS

We produced ^{92}Mo* and ^{100}Mo* compound nuclei by colliding ^{16}O on ^{76}Se at projectile energies E_{lab}=50.0 and

*Present address: Dept. of Physics, SUNY at Stony Brook, Stony Brook, NY 11794.
†Present address: Saskatchewan Accel. Lab., Univ. of Saskatchewan, Saskatoon, Saskatchewan, S7N 0W0, Canada.

TABLE I. Characteristics of the compound nuclear states populated in the present work.

Compound nucleus	Entrance channel	E^{a}_{lab} (MeV)	l_0 $\hbar$	E_{xi} (MeV)	T^{b}_{f} (MeV)	$\bar{I}^{c}$ $\hbar$
^{92}Mo	^{16}O + ^{76}Se	50.0	13.5	48.1	1.35	9.0
		72.2	29.5	66.5	1.45	19.5
^{100}Mo	^{18}O + ^{82}Se	49.1	14.0	48.1	1.35	9.3
		63.4	29.5	59.8	1.45	19.5
		72.8	36.3	67.5	1.50	24.0

[a] E_{lab} averaged over the target thickness.

[b] Estimated as in Ref. [14] based on CASCADE statistical model calculations, and using $a = A/8$ MeV^{-1}.

[c] Estimated as in Ref. [14] based on CASCADE statistical model calculations.

72.2 MeV, and ^{18}O on ^{82}Se at E_{lab}=49.1, 63.4, and 72.8 MeV, using the heavy-ion beam from the University of Washington FN tandem Van de Graaff accelerator. We used water-cooled targets of ^{76}Se (1.7 mg/cm^2) and ^{82}Se (1.0 mg/cm^2) enriched to 96.5% and 96.7%, respectively, evaporated onto platinum backings and covered with a thin layer of evaporated gold in order to reduce target degradation due to beam heating. Because the targets were backed, our useful projectile energies were limited to energies below 83 MeV, the Coulomb barrier for platinum.

Gamma rays from the decay of the compound nuclei studied were detected at a laboratory angle of 90° with respect to the beam axis, in a 25.4 cm × 25.4 cm NaI(Tl) crystal surrounded by plastic anticoincidence and lead shields. Our experimental technique was very similar to that described previously [14].

All absolute cross sections were obtained by direct calculation from the measured γ-ray yields, after correcting for pileup and dead time as described in Ref. [14]. The measured detector response was folded into the statistical model calculation for comparison with experiment.

III. RESULTS

The measured γ-ray spectra at θ_γ=90° from decays of ^{92}Mo* and ^{100}Mo* are presented in Figs. 1 and 2 (top rows), respectively. The cross-section scale was derived assuming an isotropic angular distribution. The solid curves represent statistical model calculations which are described below.

A. Statistical model analysis

Gamma-ray cross sections were calculated using a modified version of the computer code CASCADE [13] with a two-component GDR strength function. The six parameters of the GDR (peak energies E_i, widths Γ_i, and strengths S_i in units of the classical dipole sum rule; i=1,2) were treated as independent variables in a least-squares fitting of the calculated spectra to the experimental data in the high γ-ray energy range E_γ= 11.5–25 MeV. Isoscalar and isovector giant quadrupole resonances have been included in the calculations with fixed parameters based on ground-state systematics [15, 16].

In all cases the grazing angular momemtum l_0 was adjusted in order to match the magnitude of the calculated and measured spectra at low γ-ray energies, $E_\gamma \sim$ 3–6 MeV. The fusion cross sections determined in this manner are very similar to the default CASCADE cross sections except for ^{16}O + ^{76}Se at E_{lab}=72.2 MeV, for which the deduced fusion cross section was 20% smaller than the CASCADE calculation.

B. Level density

Since very little experimental information is known concerning the level density of ^{92}Mo, ^{100}Mo, and their daughters populated by compound nuclear decay, we examined the level densities for some nuclei with mass A = 85–105 calculated in the Reisdorf parametrization [12, 14, 4] and in the Pühlhofer parametrization [13, 14, 4] with parameters adjusted to reproduce the available

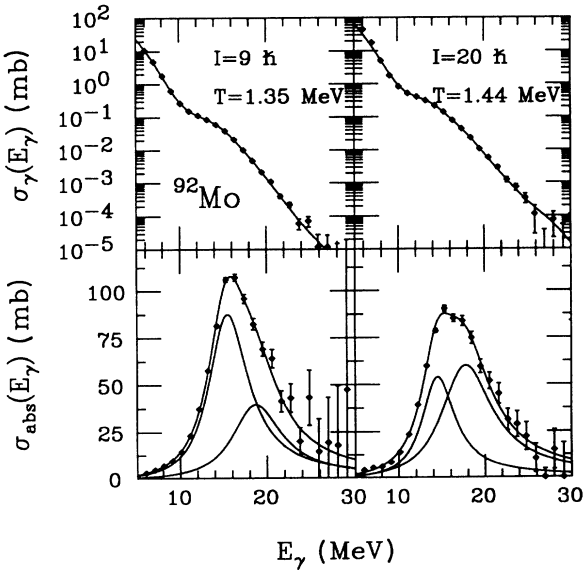

FIG. 1. Top row: measured γ-ray spectra from the decays of ^{92}Mo* together with least-squares-fitted statistical model calculations using the level density calculated in the Reisdorf parametrization. Bottom row: solid curves, fitted absorption cross section corresponding to the parameters given in Table II; data points, measured γ emission cross section $\sigma^{exp}_{\gamma}(E_\gamma)$ multiplied by the calculated ratio $\sigma_{abs}(E_\gamma)/\sigma_\gamma(E_\gamma)$.

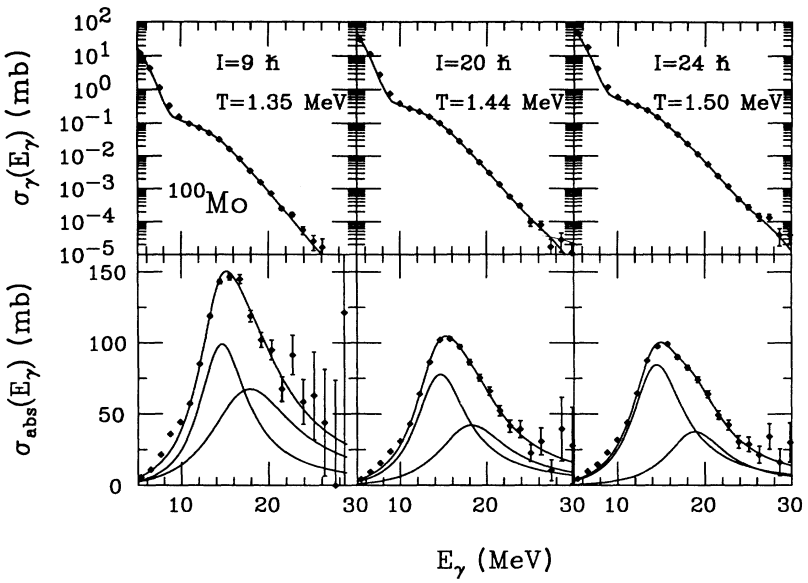

FIG. 2. The same as Fig. 1 , but for ^{100}Mo*.

experimental level spacings [17] at particular spins and particular excitation energies in the range of $6 < E_x < 12$ MeV. In the Reisdorf parametrization we used the parameters γ^{-1}=18.5 MeV, r_0=1.153 fm (corresponding to $a = A/8.70$ and $a = A/8.81$ MeV^{-1} for ^{92}Mo and ^{100}Mo, respectively) for the odd-A pairing reference as well as for the even-even pairing reference, as was found previously to be appropriate (see Fig. 4 in Ref.[4]). In the Pühlhofer parametrization the calculated level densities agree with experimental values up to energies $E_x \sim 10$ MeV, because the parameters used in the calculation have been extracted from fits to the level density data. The resulting level-density curves for the initial compound nuclei ^{92}Mo and ^{100}Mo are presented in Fig. 3. The Reisdorf approach results in a smooth energy dependence of the level density in contrast to the Pühlhofer approach, especially when $a = A/8$ MeV^{-1} is used. The level densities in the Reisdorf parametrization with the odd-A and even-even

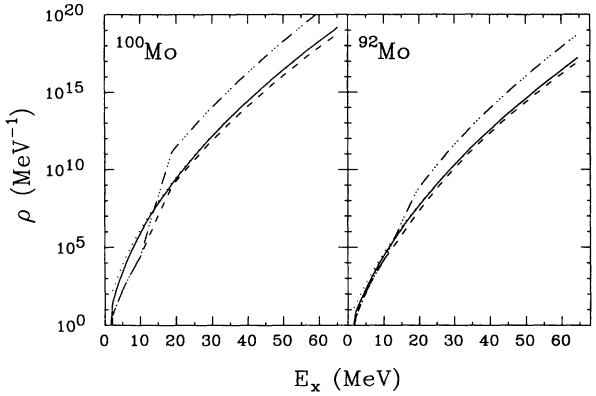

FIG. 3. Level density curves for ^{92}Mo and ^{100}Mo calculated in the Reisdorf parametrization with the best parameters for odd-A reference (solid curve), even-even reference (dots); and in the Pühlhofer parametrization with $a = A/8$ MeV^{-1} (dot-dashed curve), $a = A/9$ MeV^{-1} with the Wigner term (dashes).

reference are very close, especially above E_x=10 MeV; thus we discuss below only calculations with the odd-A reference, as was used previously [14, 4].

In Fig. 4 total level-density curves for some nuclei important in the decay of ^{92}Mo* and ^{100}Mo* calculated in the Reisdorf parametrization with γ^{-1}=18.5 MeV, r_0=1.153 fm and odd-A reference (solid curves) as well as the Pühlhofer parametrization with $a = A/8$ MeV^{-1} (dot-dashed curves) and $a = A/9$ MeV^{-1} with the Wigner term included (dashed curves) are shown together with some experimental data (solid points) from counting levels and for ^{90}Zr from the analysis of partial width fluctuations [18]. Since there is no experimental information about the level densities for nuclei of interest above $E_x \sim$12 MeV, we cannot favor any of these curves. However, the slope discontinuities present in level densities calculated for several nuclei with the Pühlhofer parametrization and $a = A/8$ MeV^{-1} may result in unreasonable GDR parameters at low bombarding energies, as has been observed previously [14, 4]. Thus, we only present here the detailed results obtained with the level densities calculated in the Reisdorf parametrization with parameters γ^{-1}=18.5 MeV, r_0=1.153 fm and odd-A pairing reference.

C. GDR parameters

In the fitting range E_γ=11.5–25 MeV, all measured spectra were well reproduced by statistical calculations with a two-component GDR strength function for each level-density parametrization discussed above. The GDR parameters extracted from the fits for the Reisdorf level-density parametrization are given in Table II. Errors in the GDR parameters include only statistics. There is an additional systematic uncertainty of ±10% in S_1+S_2 due to uncertainty in the fusion cross section. Other systematic errors are connected mainly with the uncertainty in the level density discussed above. Changing the level-density parametrization to the Pühlhofer one affects the

TABLE II. GDR parameters determined by the CASCADE fits to the measured spectra.

Compound nucleus	E_{xi} (MeV)	$\bar{E}$[a] (MeV)	E_2/E_1	S_2/S_1	S_1+S_2	Γ_1 (MeV)	Γ_2 (MeV)	FWHM[b] (MeV)
^{92}Mo	48.1	16.67±0.28	1.21±0.06	$0.56^{+0.89}_{-0.26}$	0.90±0.05	5.52±0.52	6.87 ±2.36	7.63 ±0.10
	66.5	16.58±0.15	1.23±0.03	$1.74^{+1.59}_{-0.75}$	0.90±0.05	4.68±0.84	7.31±1.17	8.60±0.20
^{100}Mo	48.1	16.38±0.47	1.22±0.36	$1.17^{+6.39}_{-0.95}$	1.63±0.28	6.70±4.36	11.48±2.70	9.79 ±0.20
	59.8	16.17±0.14	1.25±0.03	$0.75^{+3.61}_{-0.28}$	1.10±0.03	7.20±0.26	9.91±1.04	9.90±0.20
	67.5	15.96±0.24	1.30±0.02	$0.51^{+0.53}_{-0.22}$	1.03±0.03	7.16±0.48	8.19±1.61	10.06 ±0.20

[a]Mean resonance energy $\bar{E} = (E_1S_1 + E_2S_2)/(S_1 + S_2)$.

[b]Full width at half maximum calculated numerically from the fitted strength function $\sigma_{abs}(E_\gamma)$.

GDR strength S_1+S_2 by 10–20%, the mean energy $\bar{E}$ by 2–5% and the full width at half maximum (FWHM) by 1–11%.

All the fits discussed here were performed with the normal isospin-independent version of CASCADE. The fitted strengths of the GDR components were increased by 12% as estimated from CASCADE calculations which included the effect of isospin. Fits with a one-component GDR strength function were also performed. These fits yielded similar GDR strengths, mean energies lower by 0.4–0.8 MeV and widths narrower by 0.5–1.0 MeV; however, the quality of these fits was significantly worse, especially for the higher-spin cases.

The fits with a two-component GDR strength function are shown in the top rows of Figs. 1 and 2, where the measured spectra $\sigma_\gamma^{exp}(E_\gamma)$ and the fitted spectra $\sigma_\gamma(E_\gamma)$ calculated with the level densities in the Reisdorf parametrization are presented, and in the bottom rows of Figs. 1 and 2 where the photon absorption cross sections, $\sigma_{abs}(E_\gamma)$, as calculated with the GDR parameters given in Table II, are shown. In the bottom rows of Figs. 1 and 2 we display as points the quantity $\sigma_{abs}^{exp}(E_\gamma) \equiv \sigma_\gamma^{exp}(E_\gamma)\ \sigma_{abs}(E_\gamma)/\sigma_\gamma(E_\gamma)$. This quantity represents our best estimate of the photon absorption cross section

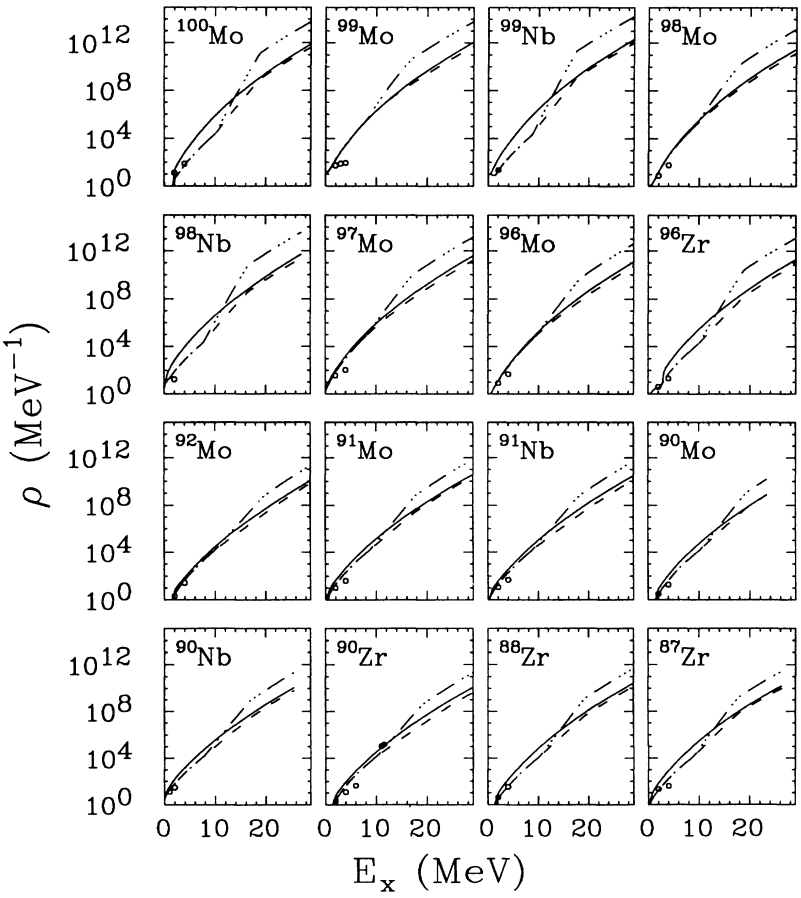

FIG. 4. Total level-density curves for some nuclei important in the decay of ^{92}Mo* and ^{100}Mo* together with the experimental data (solid points) from counting levels and from Ref. [18]. Level densities are calculated in the Reisdorf parametrization with the odd-A pairing reference and the best parameters (solid curves), and in the Pühlhofer parametrization with $a = A/8$ MeV^{-1} (dot-dashed curve), $a = A/9$ MeV^{-1} with the Wigner term (dashes).

averaged over the ensemble of states populated by GDR γ decay.

In the shape of the deduced photon absorption cross sections a broadening of the GDR in both ^{92}Mo* and ^{100}Mo* nuclei, as compared to the ground-state GDR, is clearly visible with increasing temperature and spin; however, the apparent deformation splitting is unresolved. In such cases the sense of the deformation, prolate (S_2/S_1=2) versus oblate (S_2/S_1=1/2) is difficult to determine, as is reflected by the large errors in the strength ratio S_2/S_1 for most of the fits. In particular these errors were found to be asymmetric. In Fig. 5 we show the reduced χ^2 as a function of S_2/S_1 for decay of 67.5 MeV ^{100}Mo*. The χ^2 was obtained from fits in which S_2/S_1 was fixed at various values, and for each value the other five parameters were allowed to vary. The horizontal line represents the value $\chi^2 = \chi_0^2 + 1/N_D$, where χ_0^2 is the reduced χ^2 at the minimum, and N_D is the number of degrees of freedom. In all the present cases the uncertainties in S_2/S_1 derived from the diagonal elements of the error matrix of the fit are substantially smaller than the values obtained from χ^2 plots such as Fig. 5 and thus are an underestimate of the true uncertainty when that quantity is asymmetric. From all the measured cases, only for ^{100}Mo* at E_x=67.5 MeV are the error bars small enough for the ratio S_2/S_1 to suggest the sense of the deformation, which appears to be oblate.

The total GDR strength S_1+S_2, mean energy $\bar{E}$ and full width at half maximum (FWHM) determined from the fits with a two-component GDR strength function are presented in Fig. 6 as a function of the square of the average final-state temperature T_f (see Table I). Earlier results obtained for ^{90}Zr* at $\bar{I}$ = 9$\hbar$, 22$\hbar$ and T_f=1.6, 1.7 MeV and ^{92}Mo* at $\bar{I}$=33$\hbar$ and T_f=2.0 MeV [5] are also shown here for comparison. The fitted total strength and mean energy are close to the ground-state values [9]. The GDR width increases from 5.4±0.2 MeV in the ground state to 8.6±0.2 MeV at $\bar{I}$=19.5$\hbar$, T_f=1.45 MeV for ^{92}Mo* obtained in the present work, and up to 12.1±1.0 MeV at $\bar{I}$=33$\hbar$, T_f=2.0 MeV from Ref. [5]. For ^{100}Mo* the FWHM increases from 7.9±0.2 MeV in the ground state to 9.8–10.1 MeV for $\bar{I}$=(9-24)$\hbar$ and T_f=1.35–1.50 MeV. Although both increasing spin and increasing temperature lead to a broader GDR FWHM, it appears in this temperature and spin range that the thermal broadening dominates. The data of Fig. 6 are plotted as a function of T_f^2 in order to spread out the data in a more useful manner. It is also clear that shell effects are still very important at T ~1.5 MeV, since the observed FWHM for ^{92}Mo* and ^{100}Mo* are significantly different. The rotating liquid drop model (RLDM) [19] predicts very similar, small deformations for ^{92}Mo and ^{100}Mo at the same spin (see below); thus if shell effects were absent at these temperatures, the GDR FWHM should be essentially the same in the two nuclei. The same behavior of the GDR parameters as a function of temperature and spin as shown in Fig. 6 is found when any other level-density parametrization discussed in Sec. III B is used in the calculations.

From the energy splitting of the two-component fits to the spectra, we calculate effective deformations $\beta = \frac{2}{3}\sqrt{4\pi/5}\ln(E_2/E_1)$, where E_1 and E_2 are the resonance energies for the GDR strength function components. We obtain β= 0.20±0.05 and 0.22±0.03 for the cases with average final spins 9$\hbar$ and 19.5$\hbar$ in ^{92}Mo*, and 0.21±0.27, 0.24±0.03, and 0.28±0.02 for the cases with average final spins 9$\hbar$, 19.5$\hbar$, and 24$\hbar$ in ^{100}Mo*.

From the rotating liquid drop model [19], one expects spin-induced equilibrium deformations $\beta_{\rm RLDM} \approx$ 0.01, 0.05 for ^{92}Mo at 9$\hbar$ and 19.5$\hbar$, and 0.04, 0.06 for ^{100}Mo at 19.5$\hbar$ and 24$\hbar$, respectively, and these are all much smaller than the effective deformations inferred from the data. On the other hand, the quadrupole surface softness of cold ^{92}Mo and ^{100}Mo leads to $\beta_{\rm eff} \approx$ 0.12 and 0.25, respectively, based on the $B(E2)$ values for the lowest 2^+

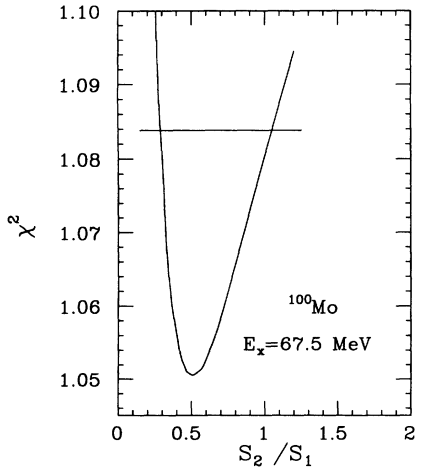

FIG. 5. The reduced χ^2 as a function of S_2/S_1. The error limits are given by the locations where the horizontal line crosses the curve.

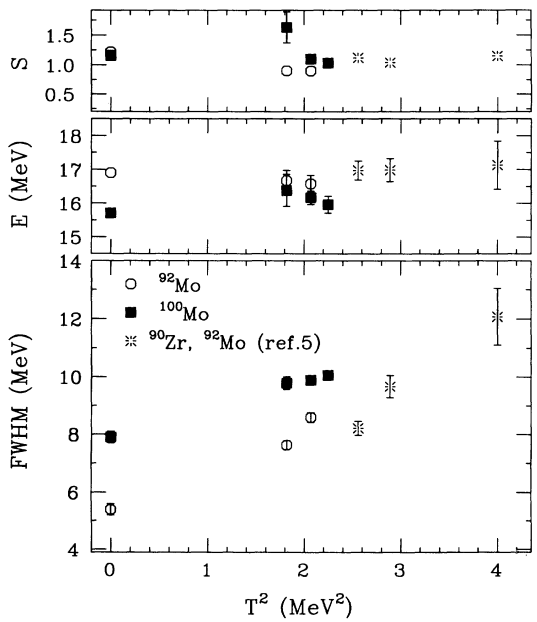

FIG. 6. The extracted GDR parameters as a function of the square of the effective temperature. Ground-state values are taken from Ref. [9].

states [20], so that large fluctuations are clearly expected for ^{100}Mo, even at very low temperatures. There is also the interesting possibility that ^{100}Mo, at the temperatures and spins of interest here, has a larger equilibrium deformation than that calculated from the RLDM, owing to its increased surface softness due to shell structure.

It is difficult to distinguish the effects of deformation fluctuations from the effects of nonzero equilibrium deformation on the γ-ray spectrum shape. Either effect can lead to an apparent two-component splitting in the GDR spectrum shape [21]. In earlier studies of ^{90}Zr* and ^{92}Mo* [5] where the γ-ray spectra as well as the angular distributions were measured at mean spins and temperatures in the range (9–33)$\hbar$ and 1.6–2 MeV, respectively, and compared with theoretical calculations including intrinsic-shape fluctuations and shape-orientation fluctuations [22], it was found that large thermal shape fluctuations are present at this spin and temperature, which accounted for the observed spectral shapes. In these cases the deformations inferred from the energy splittings were larger than the equilibrium deformations but smaller than the most probable deformations (due to fluctuations). Since the energy splittings are comparable in these two experiments, a similar explanation may apply to the present results.

An extrapolation of the data of Fig. 6 suggests that at $T_f^2 \sim 3$–4 MeV^2 ($T_f \sim 1.7$–2 MeV) the GDR FWHM for ^{100}Mo* and ^{92}Mo* would be similar, which further suggests that shell effects may no longer be significant at these temperatures, in accord with conventional expectation. However, since the thermal fluctuations increase with temperature, the same shell effects in the nuclear potential energy surface may lead to a smaller FWHM difference for ^{92,100}Mo* at high temperature than at low temperature. Indeed, if we (crudely) estimate the additional broadening in ^{100}Mo compared to ^{92}Mo as $\Delta \equiv \sqrt{[\mathrm{FWHM}(^{100}\mathrm{Mo}^*)]^2 - [\mathrm{FWHM}(^{92}\mathrm{Mo}^*)]^2}$; i.e., we fold in quadrature the FWHM in ^{92}Mo with Δ in order to obtain the FWHM in ^{100}Mo, then Δ= 5.8, 6.1, 4.9 MeV for T_f= 0, 1.35, 1.45 MeV, respectively. Thus if we identify Δ as a measure of the effect of shell corrections on the GDR FWHM difference, then there is no evidence that shell corrections have changed significantly over this temperature range.

IV. CONCLUSION

Over the temperature and spin range of the present study the GDR FWHM for decay of ^{100}Mo* is consistently larger than the FWHM for decay of ^{92}Mo* as is also observed for the GDR built on the ground state. This clearly indicates the persistence of shell effects up to a temperature $T \approx 1.5$ MeV, the highest temperature studied. From these results alone, it is not clear whether shell effects are similar or are reduced relative to zero temperature.

From general considerations (see, e.g., Ref. [8] , Fig. 6-54) one expects a reduction of a factor of 3.5–4.5 in the contribution of the shell correction to the free energy at T = 1.5 MeV relative to that at T = 0. A similar reduction factor of 4.5 is expected from the Reisdorf level density prescription, in which the shell correction is exponentially damped with a damping factor γ^{-1}= 18.5 MeV (see above). It seems surprising that such a large GDR FWHM difference as is observed in the present experiment would result from shell corrections at $T \approx 1.5$ MeV which are only 20–25% as large as at T=0.

The shell corrections could be determined by comparing the present results with detailed thermal averaging calculations based on Strutinsky shell-corrected potential energy surfaces. Such calculations have been performed for other cases, and generally account well for the observed FWHM [23]; unfortunately the present cases have not yet been calculated.

ACKNOWLEDGMENTS

One of us (M.K.-H.) would like to thank the members of the University of Washington Nuclear Physics Laboratory for their generous hospitality. Financial support from the U.S. Department of Energy and from the Polish Ministry of National Education (under Contract No. CPBP 01.06) is gratefully acknowledged.

[1] C. A. Gossett, K. A. Snover, J. A. Behr, G. Feldman, and J. Osborne, Phys. Rev. Lett. **54**, 1486 (1985).

[2] P. Thirolf, D. Habs, D. Schwalm, R. D. Fisher, and V. Metag, in *Proceedings of the First Topical Meeting on Giant Resonance Excitation in Heavy Ion Collisions*, edited by P. F. Bortignon, J. J. Gaardhøje, and M. DiToro, Legnaro, Italy, 1987 [Nucl. Phys. **A482**, 93c (1988)].

[3] A. M. Bruce, J. J. Gaardhoje, B. Herskind, R. Chapman, J. C. Lisle, F. Khazaie, J. N. Mo, and P. J. Twin, Phys. Lett. B **215**, 237 (1988).

[4] M. Kicińska-Habior, K. A. Snover, J. A. Behr, G. Feldman, C. A. Gossett, and J. H. Gundlach, Phys. Rev. C **41**, 2075 (1990).

[5] J. H. Gundlach, K. A. Snover, J. A. Behr, C. A. Gossett, M. Kicińska-Habior, and K. T. Lesko, Phys. Rev. Lett. **65**, 2523 (1990).

[6] J. J. Gaardhoje and A. Maj, Nucl. Phys. **A520**, 575c (1990).

[7] J. Hadermann and A. C. Rester, Nucl. Phys. **A231**, 120 (1974).

[8] A. Bohr and B. R. Mottelson, *Nuclear Structure* (Benjamin, New York, 1975), Vol. II, Chap. 6.

[9] H. Beil, R. Bergere, P. Carlos, A. Lepretre, A. de Miniac and A. Veyssiere, Nucl. Phys. **A227**, 427 (1974).

[10] T. J. Bowles, R. J. Holt, H. E. Jackson, R. M. Laszewski, R. D. McKeown, A. M. Nathan, and J. R. Specht, Phys. Rev. C **24**, 1940 (1981).

[11] M. G. Huber, M. Danos, H. J. Weber, and W. Greiner, Phys. Rev. **155**, 1073 (1967).

[12] W. Reisdorf, Z. Phys. A **300**, 227 (1981).

[13] F. Pühlhofer, Nucl. Phys. **A280**, 267 (1977).
[14] M. Kicińska-Habior, K. A. Snover, C. A. Gossett, J. A. Behr, G. Feldman, H. K. Glatzel, and J. H. Gundlach, Phys. Rev. C **36**, 612 (1987).
[15] F. E. Bertrand, Annu. Rev. Nucl. Sci. **26**, 457 (1976).
[16] B. L. Berman and S. C. Fultz, Rev. Mod. Phys. **47**, 713 (1975).
[17] W. Dilg, W. Schantl, H. Vonach, and M. Uhl, Nucl. Phys. **A217**, 269 (1973).
[18] A. Dygo, G. Szeflińska, Z. Szefliński, and Z. Wilhelmi, Nucl. Phys. **A378**, 293 (1982).
[19] S. Cohen, F. Plasil, and W. J. Swiatecki, Ann. Phys. (N.Y.) **82**, 557 (1974).
[20] P. H. Stelson and L. Grodzins, Nucl. Data **1**, 21 (1965).
[21] K. A. Snover, in *Proceedings of the First Topical Meeting on Giant Resonance Excitation in Heavy Ion Collisions*, Legnaro, Italy, 1987 [Nucl. Phys. **A482**, 13c (1988)].
[22] Y. Alhassid and B. Bush, Phys. Rev. Lett. **65**, 2527 (1990).
[23] Y. Alhassid and B. Bush, Nucl. Phys. **A514**, 434 (1990).